Selective oxidation of propylene by O_2 with visible light in a zeolite

Fritz Blatter, Hai Sun and Heinz Frei [1]

Laboratory of Chemical Biodynamics, Lawrence Berkeley Laboratory, University of California, Berkeley, CA 94720, USA

Received 10 April 1995; accepted 11 July 1995

Propylene and O_2 loaded into zeolite BaY were found to react upon irradiation with green or blue light in a single photon process. In situ monitoring by FT-infrared spectroscopy showed that allyl hydroperoxide is the predominant product at −100°C. At room temperature, acrolein, propylene oxide, and allyl hydroperoxide were observed in comparable amounts. The aldehyde and epoxide are shown to emerge from secondary thermal chemistry of the allyl hydroperoxide photoproduct. The selectivity in terms of the hydroperoxide photoproduct is very high (98% at room temperature) even at high propylene conversion. Diffuse reflectance spectra show that access to the mild oxidation path is made possible by a zeolite-induced shift of the propylene·O_2 charge-transfer absorption from the UV into the visible region.

Keywords: propylene–oxygen photochemistry; selective propylene oxidation; zeolite BaY; propylene-to-acrolein conversion; allyl hydroperoxide

1. Introduction

Oxidation by O_2 is the single most important process for the conversion of abundant hydrocarbons to industrially useful oxygenated derivatives such as building blocks for the manufacture of plastics and synthetic fibers [1–3]. In large-scale synthesis the use of molecular oxygen as oxidant is dictated primarily by economic factors. Even for oxidation processes on a moderate scale, O_2 is increasingly favored over other, more expensive oxidants because of environmental considerations. Yet autoxidation of abundant hydrocarbons, especially small olefins, is inherently unselective, whether conducted in the gas or liquid phase, or whether catalyzed by transition metals or not [2]. One reason is that the chain reaction leading to the primary product, an allyl hydroperoxide, is diverted by termination steps which result in the formation of oxy radicals. These highly reactive species can undergo several competing reactions that are very difficult to control. The result is a multitude of

[1] To whom correspondence should be addressed.

© J.C. Baltzer AG, Science Publishers

products which includes alcohols, carbonyl compounds, and epoxides [2,4]. Furthermore, initial products such as alcohols, epoxides, and carbonyls are more easily oxidized by O_2 than the parent alkene under thermal conditions. Therefore, oxidations by O_2 exhibit most often little chemo- or regioselectivity. Formation of the most stable oxidation product, CO_2, cannot be avoided in many cases. As a consequence, conversions have to be kept low (at a few percent). However, in the case of alkenes with less than five carbons, selectivities are poor even at very low conversion [2,4]. A major challenge in the field of olefin + O_2 chemistry is, therefore, to find reaction paths that afford the primary hydroperoxide product with high selectivity at high conversion.

We report here a method that affords selective conversion of propylene by O_2 to the hydroperoxide intermediate for the first time. The approach is based on photoexcitation of the propylene·O_2 charge-transfer state in a zeolite. The molecular-size cages of the latter offer a natural environment for the formation of alkene·O_2 collisional pairs at high concentration. The key to selectivity lies in a low-energy reaction path that can be accessed by visible photons. This path is opened up by a very strong stabilization of the excited charge-transfer state by the high electrostatic field of the zeolite matrix cage which we found recently while studying the photooxidation of higher alkenes [5–7] and of toluene [8]. Access to this low-energy excited state, coupled with the positional constraint imposed by the zeolite nanocage [9] furnishes a new, controlled reaction path for this prototype alkene + O_2 system.

2. Experimental

Zeolite BaY was prepared by repeated ion exchange of NaY (Aldrich, Lot #03319TX) at 90°C in a 0.5 M solution of $BaCl_2$. The degree of ion exchange was determined by dissolution of the zeolite in 40% hydrofluoric acid and recording of the Na, Ba, and Al content by inductively-coupled plasma atomic emission spectroscopy. Ninety-seven percent of Na^+ was exchanged. Self-supporting zeolite wafers of 10 mg (1.2 cm diameter) were placed in a miniature infrared or UV-Vis vacuum cell described previously [6,7]. For infrared measurements, the cell was mounted inside a variable temperature vacuum system [5,6,8]. The zeolite was dehydrated by heating the cell to 200°C for 12–15 h while evacuating with a turbomolecular pump. The loading level of the reactants depended on the gas pressure of the reactants and the zeolite temperature.

Photochemistry was monitored in situ by Fourier-transform infrared (FT-IR) spectroscopy using a Bruker model IFS 113 instrument. Zeolite BaY is transparent in the infrared except for the region 1200–920 cm^{-1}, and below 800 cm^{-1}. For photolysis, a prism tuned Ar ion laser Coherent model Innova 90-6 or the emission of a tungsten lamp was used. The photolysis light beam was expanded to cover the entire pellet. Experiments were conducted at temperatures between −100 and

21°C. Diffuse reflectance spectra in the UV-Vis region were recorded with a spectrometer Shimadzu model 2100 with an integrating sphere set-up model ISR-260.

Oxygen (Air Products, 99.997%) was used as received. Propylene (Matheson, 99.5%), acrolein (Aldrich, 90%), allyl alcohol (Aldrich, 99%), and propylene oxide (Aldrich, 99%) were vacuum-distilled prior to use.

3. Results and discussion

A faujasite type Y zeolite was chosen for the photochemistry because this material can be prepared in very pure form. It consists of a three-dimensional network of spherical nanocages (13 Å diameter, 8 Å windows), called supercages [9]. Among the type Y zeolites that are free of Lewis and Brønsted acid sites, the Ba^{2+}-exchanged form exhibited the highest photochemical reaction yields and was therefore used primarily. Loading of propylene from the gas phase into dehydrated zeolite BaY could readily be monitored in situ by FT-IR spectroscopy. The top trace of fig. 1 shows the infrared absorptions of $CH_2{=}CH{-}CH_3$ in the zeolite in the 1750–800 cm^{-1} region. In this experiment the loading pressure of the alkene was 3 Torr and the matrix was held at −100°C. This resulted, on average, in four propylene molecules per supercage. Subsequent exposure to 700 Torr O_2 gas added four oxygens to each supercage [9]. Chemical reaction was observed upon irradiation of the zeolite pellet with blue continuous-wave laser light ($\lambda = 488$ nm). This is manifested by the reactant depletion and product growth in the infrared difference spectrum displayed in fig. 1B. Reaction could also be induced by excitation with 514 nm green light. Product growth was linear in laser intensity. Laser heating effects were less than 10°C [6,8]. Monochromatic laser light was employed in order to determine the wavelength responsible for the observed photochemistry. However, the chemistry could be initiated equally well with visible light from a conventional tungsten lamp. In this case, a Corning glass filter (No. 3-72) ensured that only emission at $\lambda > 430$ nm impinged on the zeolite. Product spectra and yields were found to be independent of the photolysis source. Fig. 2 shows the result of an irradiation experiment with the tungsten source in which the zeolite matrix was held at room temperature.

Comparison of the experiments at room temperature (fig. 2) and at −100°C (fig. 1B) allowed us to elucidate the photochemical reaction path. Readily identified products in the room temperature zeolite are acrolein (propenal, e.g. the strong C=O stretching absorption at 1670 cm^{-1}) and allyl hydroperoxide (e.g. the band at 1419 cm^{-1}). At −100°C, allyl hydroperoxide was trapped as the main product. At this low temperature the hydroperoxide is stable, in contrast to the situation at room temperature. The growth of even the most prominent acrolein band at 1670 cm^{-1} is very small, indicating that only a minute amount is formed. On the other hand, growth of some propylene oxide (methyloxirane) is manifested by char-

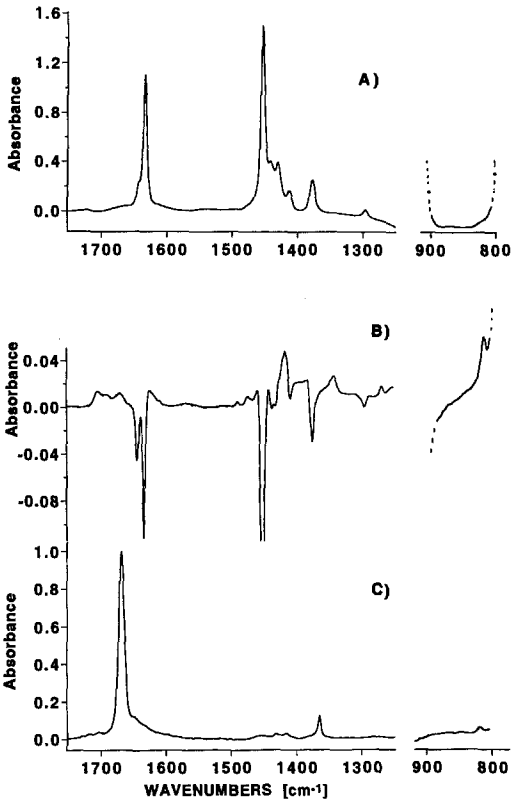

Fig. 1. Visible light-induced reaction of propylene with O_2 in zeolite BaY at $-100°C$ monitored by FT-IR spectroscopy. (A) Difference spectrum before and after loading of propylene and O_2. (B) Difference spectrum following irradiation at 488 nm (400 mW cm^{-2}) for 300 min. (C) Difference spectrum following warm-up of the photolysis product allyl hydroperoxide (accumulated in experiment (B)) to room temperature. Note that the long photolysis times are required because of the strong visible light scattering of the zeolite pellet and not because of a low reaction quantum efficiency, as explained in the text.

acteristic bands at 1490, 1268, and 820 cm^{-1}. Complete product spectra, including ^{18}O and D isotope frequency shifts, are presented in table 1.

In order to find out about the origin of acrolein and propylene oxide, and to establish means to control the formation of these products, allyl hydroperoxide was accumulated at $-100°C$. In one experiment, the remaining propylene and O_2 was then selectively removed from the zeolite cages by evacuation. Subsequent warm-up of the matrix to room temperature resulted in quantitative rearrangement of the allyl hydroperoxide to acrolein under elimination of water (fig. 1C). The half-life of the hydroperoxide in BaY at 21°C is about 6 h. This thermal process explains why the acrolein to allyl hydroperoxide branching ratio is much larger when conducting the photochemistry at temperatures above $-100°C$, and reveals the origin of the product. When conducting the warm-up of allyl hydroperoxide in the pres-

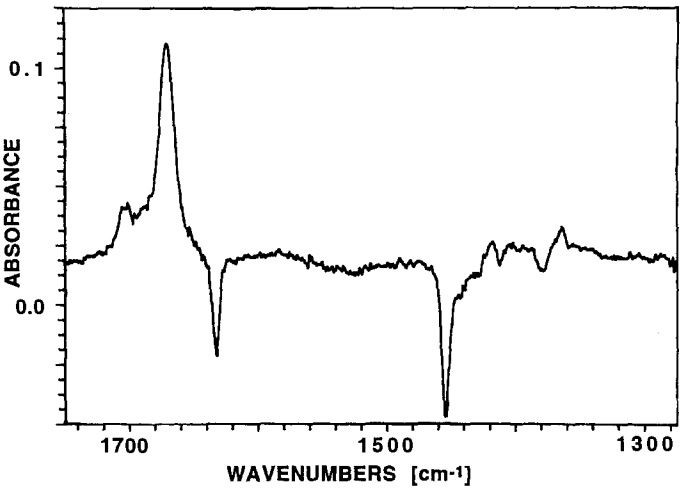

Fig. 2. FT-IR difference spectrum of propylene + O_2 photochemistry in zeolite BaY at room temperature. The reaction was induced by the visible emission of a tungsten lamp for 180 min at 200 mW cm^{-2}. Loading levels are three propylene molecules per supercage and one O_2 per five supercages on average.

ence of excess propylene, propylene oxide grew in under concurrent depletion of the hydroperoxide and the olefin. In fact, thermal epoxidation of excess propylene by allyl hydroperoxide proceeded slowly even at −100°C during and after photoaccumulation of CH_2=CH−CH_2OOH. The small growth of propylene oxide in fig. 1B is attributed to this secondary, thermal process. We conclude that the epoxide, like acrolein, is a secondary product formed by thermal O transfer from CH_2=CH−CH_2OOH to CH_2=CH−CH_3. The secondary reaction behavior was also manifested in the distinct growth kinetics of these two products. An induction period was observed for both products, which was most pronounced in the case of the propylene-d_6 + O_2 system. No distinct infrared absorptions of the expected allyl alcohol coproduct (CH_2=CH−CH_2OH) could be detected. This is nonetheless consistent with CH_2=CH−CH_2OH growth since spectra of authentic samples of allyl alcohol in BaY showed that all infrared bands overlap with intense propylene or product absorptions (we did observe the corresponding alcohol product in the case of butene + O_2 system [6]). Aside from allyl hydroperoxide and its secondary products, acrolein and propylene oxide, weak bands at 2848, 1705, and 1502 cm^{-1} point to the formation of small amounts of formaldehyde and acetaldehyde (table 1).

The photochemical step of the propylene + O_2 reaction is highly selective. At room temperature 98% of the reactants form allyl hydroperoxide intermediate. If we run the photochemistry at −100°C, 99.8% of the reacting propylene gives the hydroperoxide initially. These results are further detailed in table 2. The branching between subsequent rearrangement of the hydroperoxide to acrolein, and O transfer to excess propylene depends on temperature and olefin concentration. Table 3

Table 1
Observed infrared product absorptions

$C_3H_6 + O_2(^{18}O_2)$ (cm^{-1})	$C_3D_6 + O_2(^{18}O_2)$ (cm^{-1})	Assignment [a]
820 [b]		PO
(889) [c]	(887) [c]	AHP, PO
1268 (−2)	1270 (0)	PO
1282 (−1)		ACR
1343 (−3)	1367 (−1)	AHP
1364 (−3)		ACR
1415 (−2)		ACR
1419 (−1)		AHP
	1423	HDO
1430 (−3)		ACR
	1442	HDO
1450 ± 10 [d]		AHP, PO
1473 (−3)		AHP
1490 (−3)		PO
1502 (−1)		CH_2=O
1640 (−3)	1581 (−1)	AHP
1649 [e]		H_2O
1670 (−21)	1649 (−25)	ACR
1705 (−30)	1666 [e]	CH_2=O
	1685 (−31)	CH_3CH=O
2848		CH_2=O
3000	2221	AHP
3065	2300 [f]	AHP, HDO
3450 [f]		H_2O

[a] PO, propylene oxide; AHP, allyl hydroperoxide; ACR, acrolein. Identification of AHP is based on the ^{18}O and D isotope frequency shifts and the agreement with reported infrared spectra [10]. Acrolein, propylene oxide, acetaldehyde, and formaldehyde were identified by recording spectra of authentic samples in BaY. In the case of CH_2=O and CH_3CH=O, a 1 : 1 mixture of the two species, loaded into BaY, reproduced the relative intensities of the 2848, 1705, and 1502 cm^{-1} bands. The absence of other CH_2=O and CH_3CH=O bands is consistent with their much lower absorption cross sections.

[b] Absorption of the ^{18}O-labeled product obscured by zeolite absorption (red shift > 15 cm^{-1}).

[c] Only the ^{18}O-labeled product band could be observed. The parent product absorption is overlapped by zeolite absorption at $\tilde{\nu} > 900$ cm^{-1}.

[d] This band is overlapped by an intense (decreasing) propylene absorption.

[e] The ^{18}O-frequency shift cannot be determined due to overlap with the intense ν(CO) absorption of acrolein-^{18}O.

[f] Very broad, FWHM ≈ 400 cm^{-1}.

shows the product ratios at −100 and 0°C. At the lower temperature, trapped allyl hydroperoxide is the overwhelming product while at 0°C the hydroperoxide, propylene oxide, and acrolein appear in close to equal amounts. It is striking that the formation of acrolein is much more sensitive to temperature than the epoxidation reaction. Hence, the branching between the important industrial intermediates

Table 2
Selectivity of propylene + O_2 photoreaction in BaY

Photolysis product	$C_3H_6 + O_2$ at −100°C (yield in %)	$C_3H_6 + O_2$ at 0°C (yield in %)	$C_3D_6 + O_2$ at 0°C (yield in %)
total allyl hydroperoxide [a]	99.8 ± 0.2	98 ± 1	96 ± 2
total aldehyde [b]	0.2 ± 0.2	2 ± 1	4 ± 2

[a] AHP + ACR + PO.
[b] $CH_2{=}O + CH_3CH{=}O$.

acrolein and propylene oxide can be controlled by the temperature and the level of excess propylene admitted to the zeolite. This is very different from thermal propylene autoxidation where already at the chain propagation stage nearly half of the intermediates are diverted to form alkoxy and polyperoxy radicals [2]. Moreover, the subsequent thermal chemistry of the allyl hydroperoxide intermediate involves homolytic OO bond rupture resulting in additional formation of energetic radicals that react indiscriminately.

A crucial result is that the high selectivity in terms of allyl hydroperoxide as primary product holds even at high conversion of propylene. Reaction leveled off after about 20% of the propylene loaded into the zeolite had been consumed. This is due to the strong scattering of the photolysis light by the BaY pellet (see below) which limits penetration of visible light to approximately one quarter of the zeolite volume. The conversion with respect to the propylene residing in the irradiated section of BaY is around 80%.

While there is a commercially important method for propylene to acrolein oxidation by O_2 using a Bi molybdate catalyst [11], no selective conversion of propylene to propylene oxide by oxygen through thermal catalysis has been reported thus far. Selective propylene epoxidation schemes use H_2O_2 or organic hydroperoxides as O donors [1,2]. A recent breakthrough is the use of zeolite catalysts (Ti-silicalite) for epoxidation by H_2O_2 [12].

The optical absorption responsible for the visible photochemistry is shown in fig. 3 in the form of a diffuse reflectance spectrum. The curve represents the ratio of the reflectance of propylene-loaded BaY after and before exposure to 700 Torr

Table 3
Distribution between trapped allyl hydroperoxide and its thermal products

Product	$C_3H_6 + O_2$ at −100°C [a] (yield in %)	$C_3H_6 + O_2$ at 0°C [b] (yield in %)
allyl hydroperoxide	86.5 ± 1	38 ± 2
acrolein	0.2 ± 0.1	24 ± 2
propylene oxide	13 ± 1	36 ± 2

[a] Four propylene molecules per supercage.
[b] Three propylene molecules per supercage.

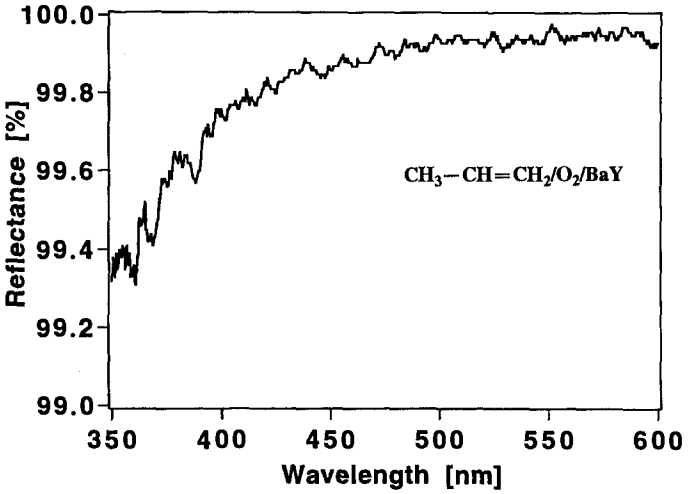

Fig. 3. Visible/UV diffuse reflectance spectrum of propylene and O_2-loaded zeolite BaY at room temperature. Reflection of visible light by the pellet is highly diffuse because the zeolite Y crystals have an average size of about one micron [9].

O_2 gas. The band appeared only when propylene and O_2 were simultaneously present in the zeolite, and it could be reversibly removed by pumping off the oxygen. This demonstrates that the absorption originates from a propylene·oxygen complex. We assign the band to a propylene·O_2 charge-transfer transition. This is supported by our observation of analogous alkene·O_2 absorptions for 2-butene, 2-methyl-2-butene, and 2,3-dimethyl-2-butene in zeolite NaY and BaY [5–7]. The onset increases with the ionization potential of the olefin in agreement with Mulliken's theory of charge-transfer transitions [13]. The propylene·O_2 absorption shown in fig. 3 fits well into this trend. This is best illustrated by the agreement of the ionization potential difference between cis- or trans-2-butene (9.13 eV) and propylene (9.73 eV) on the one hand, and the observed 100 nm blue shift of the propylene·O_2 absorption onset relative to 2-butene·O_2 on the other (BaY) [6,7]. The onset of the propylene·O_2 charge-transfer absorption in the gas phase and in solid O_2 is at 270 nm [14,15]. The threshold in BaY is around 500 nm, which implies a 17 000 cm^{-1} (2.1 eV) red shift of the charge-transfer band by the zeolite cage environment. This shift is unprecedented for a hydrocarbon·O_2 charge-transfer band and exceeds red shifts of charge-transfer bands of neutral donor–acceptor complexes in polar solvents by at least an order of magnitude [16].

An alternative explanation of the visible absorption in terms of an O_2-enhanced triplet absorption of propylene is ruled out because the lowest triplet state of the olefin lies in the UV region. Phosphorescence studies have shown that spectral shifts of triplet states upon loading of simple organics into zeolites are small [17].

The 13 Å supercages of zeolite Y carry a formal negative charge of 7. This charge resides on the framework oxygen atoms and is counterbalanced by three to four

Ba^{2+} ions per cage [9]. BaY is a special case among the alkaline earth zeolites Y in that all cations are located in the supercages. This is because the size of Ba^{2+} is too large to enter the smaller sodalite or double 6-ring cavities [9]. Electric shielding of the cations by the framework oxygens in the supercage is poor. We have obtained evidence for electrostatic fields of the order of 0.5 V $Å^{-1}$ by measurement of induced infrared bands of O_2 and N_2 stretch fundamentals in BaY [18]. This method of determining electrostatic fields in zeolites was first introduced by Cohen de Lara in studies on zeolite A [19]. Fields on the order of one to several V $Å^{-1}$ at distances up to several Å from the cation have been predicted by model calculations [9]. Furthermore, ESR spectroscopy of guest radicals in alkali-exchanged zeolite Y indicates fields in the range 0.2–1 V $Å^{-1}$ [20,21]. Among the potential energy terms describing the interaction of the alkene·O_2 complex with the zeolite matrix cage (electrostatic, induction, dispersion, repulsion), the electrostatic field–dipole interaction ($-\boldsymbol{\mu} \cdot \boldsymbol{E}$) is expected to be most strongly affected by excitation of the charge-transfer state. Photoexcitation is accompanied by the development of a large dipole across the reactant complex because of the charge separation. Assuming a separation of the alkene$^+$·O_2^- charge centers of 4 Å and an electrostatic field of 0.5 V $Å^{-1}$, we calculate a dipole stabilization of 2.0 eV. We attribute the large red shift of the charge-transfer band to this electrostatic field effect. While a quantitative prediction of the charge-transfer state energy and the shape of the absorption band will require a quantum chemical treatment of the alkene·O_2-zeolite interaction, this estimate nonetheless shows that the expected dipole stabilization is in the range of the observed red shift of the absorption onset.

The quantum yield of reaction is equal to the product growth per absorbed photon. The number of product molecules generated was measured by the infrared absorbance growth, while the number of photolysis quanta absorbed by the charge-transfer band was determined from the spectrum fig. 3. A rather high reaction quantum efficiency of 20% was estimated. The reaction rate is equal to the product of quantum yield, light source intensity, and fraction of light absorbed by the reactants. Hence, a lamp with 100 W power in the range 400–500 nm, focussed on a 1 cm^2 area of a zeolite pellet, would generate 0.25 mmol oxidation product per hour if the pellet is 20 μm thick, or between 0.1 and 0.2 mol per hour for a pellet thickness of 1 mm (we estimate that the penetration of visible light in our pellets is limited to about 20 μm because of strong light scattering by the one-micron crystallites. Note that the low absorption in fig. 3 is due to the light scattering rather than a vanishing extinction coefficient of the propylene·O_2 charge-transfer absorption). Optically transparent zeolite membranes will be needed to accomplish photolysis in millimeter-type layers.

Scheme 1 shows the proposed reaction mechanism. Upon excitation of the propylene·O_2 charge-transfer state, proton transfer to O_2^- results in the formation of an allyl/O_2H radical pair in the zeolite cage. Combination of the radical pair would give the observed allyl hydroperoxide. This mechanism is consistent with the fact that alkene radical cations are extremely acidic ($pK_a \leqslant 0$) [22]. We consider

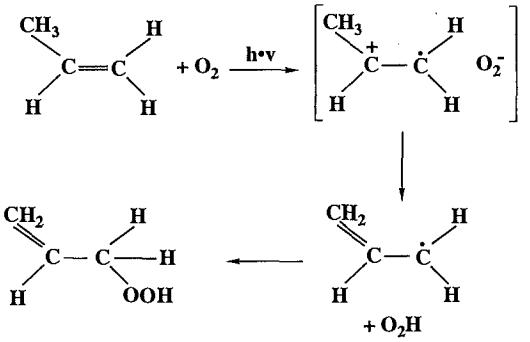

Scheme 1.

the fast deprotonation of the propylene radical cation as the key to the rather high quantum yield of reaction; the proton transfer from the cation to O_2^- competes effectively with back electron transfer, probably also because the latter falls within the inverted Marcus region and hence is slow. Traces of acetaldehyde and formaldehyde are attributed to fragmentation of transient methyl dioxetane formed by direct addition of O_2^- and $C_3H_6^+$ radical ions. This is consistent with the observed D isotope effect on the product branching shown in table 2. Dioxetane formation has a precedent in the electron-transfer sensitized photooxidation of olefins by dyes [23].

4. Conclusions

In summary, several factors contribute to the tight control of the photochemical propylene oxidation pathway in terms of allyl hydroperoxide formation. The principal factor is the very strong stabilization of the excited alkene·oxygen charge-transfer state by the electrostatic field of the zeolite matrix cage. The charge-transfer state can be accessed by low-energy visible instead of the more energetic UV photons, with the result that primary products emerge with minimal excess energy. This, coupled with the confinement imposed by the zeolite cage, prevents random radical coupling reactions and homolytic fragmentation of the primary products. Moreover, the use of visible light ensures that no photodissociation or further oxidation of acrolein or propylene oxide by O_2 can occur. The ionization potential increases upon partial oxidation of the alkene (9.73 eV for propylene, 10.10 eV for acrolein, 10.22 eV for propylene oxide). The result is that the onset of the charge-transfer absorption of acrolein·O_2 and propylene oxide·O_2 complexes lies at shorter wavelengths than in the case of the propylene·O_2 system, which renders secondary photooxidation of the primary products unlikely. Hence, the photochemical method of alkene oxidation by O_2 is inherently stable against reaction of primary products with oxygen. The temperature and concentration dependence of

the acrolein to propylene oxide branching furnishes a means to manipulate the final oxidation product ratio, and work on this aspect is in progress.

The fact that photochemical reactions without added sensitizer usually require UV light is among the foremost reasons why direct (sensitizer-free) photochemical methods have thus far played no role in the practical synthesis of small organics in general, and in oxidation of abundant hydrocarbons in particular (photosensitized oxidation of alkenes with singlet oxygen ($O_2(^1\Delta)$) can lead to allyl hydroperoxides in high yield; however, this reaction does not work for terminal and small alkenes ($< C_5$)) [24]. Photochemistry in zeolites with inexpensive visible light at (or close to) ambient temperature may open up transformations of unfunctionalized alkanes, alkenes, and aromatics by molecular oxygen to important industrial organics in a selective and benign way, a long-standing goal in the field of hydrocarbon oxidation.

Acknowledgement

This work was supported by the Director, Office of Energy Research, Office of Basic Energy Sciences, Chemical Sciences Division, of the US Department of Energy under Contract No. DE-AC03-76SF00098.

References

[1] R.A. Sheldon and J. Dakka, Catal. Today 19 (1994) 215.
[2] R.A. Sheldon and J.K. Kochi, *Metal-Catalyzed Oxidation of Organic Compounds* (Academic Press, New York, 1981).
[3] G.W. Parshall and S.D. Ittel, *Homogeneous Catalysis*, 2nd Ed. (Wiley, New York, 1992).
[4] R.A. Sheldon, in: *The Chemistry of Functional Groups – Peroxides*, ed. S. Patai (Wiley, New York, 1983) ch. 6.
[5] F. Blatter and H. Frei, J. Am. Chem. Soc. 115 (1993) 7501.
[6] F. Blatter and H. Frei, J. Am. Chem. Soc. 116 (1994) 1812.
[7] F. Blatter, F. Moreau and H. Frei, J. Phys. Chem. 98 (1994) 13403.
[8] H. Sun, F. Blatter and H. Frei, J. Am. Chem. Soc. 116 (1994) 7951.
[9] D.W. Breck, *Zeolite Molecular Sieves: Structure, Chemistry, and Use* (Wiley, New York, 1974).
[10] S. Dykstra and H. Mosher, J. Am. Chem. Soc. 79 (1957) 3474.
[11] R.K. Grasselli, G. Centi and F. Trifirò, Appl. Catal. 57 (1990) 149.
[12] B. Notari, Stud. Surf. Sci. Catal. 37 (1987) 413.
[13] R.S. Mulliken and W.B. Pearson, *Molecular Complexes* (Wiley, New York, 1969).
[14] M. Itoh and R.S. Mulliken, J. Phys. Chem. 73 (1969) 4332.
[15] S. Hashimoto and H. Akimoto, J. Phys. Chem. 91 (1987) 1347.
[16] C. Reichardt, *Solvent Effects in Organic Chemistry* (Verlag Chemie, Weinheim, 1979).
[17] V. Ramamurthy, in: *Photochemistry in Organized and Constrained Media*, ed. V. Ramamurthy (VCH Publishers, New York, 1991) ch. 10.
[18] F. Blatter and H. Frei, to be submitted.
[19] B. Barrachin and E. Cohen de Lara, J. Chem. Soc. Faraday Trans II 82 (1986) 1953.

[20] J.A.R. Coope, C.L. Gardner, C.A. McDowell and A.I. Pelman, Mol. Phys. 21 (1971) 1043.
[21] H. Sugihara, K. Shimokoshi and I. Yasumori, J. Phys. Chem. 81 (1977) 669.
[22] O. Hammerich and V.D. Parker, Adv. Phys. Org. Chem. 20 (1984) 55.
[23] C.S. Foote, Tetrahedron 41 (1985) 2221.
[24] H.H. Wasserman and R.W. Murray, *Singlet Oxygen* (Academic Press, New York, 1979).